Selective Detection of Simple and Double Grounding within the Medium Voltage Electrical Networks with Compensated Null

D. Toader, P. Ruset, I. Hategan *IEEE Member*, I. Diaconu, N. Pinte

***Abstract* — This paper was written after some tests for default detection in MV network with compensated neutral in Romania. The results after these experiments are presented in comparison with numerical simulation. The results of this research are put into practice through a hardware device BZCD - 2 as digital protection block. The experimental determination has demonstrated very good reaction of this protection.**

***Index Terms* — current harmonics module, digital protection block, homopolar capacitive impedance, simple grounding fault.**

I. Introduction

The problem for selective detection of simple, respectively double grounding within the medium voltage electrical networks from Romania has represented and still represents a concern for many specialists in the power field. The development of the numerical protection equipments from the past years represents an important requirement for achieving selective protections which would allow extending the possibilities to discover the above mentioned defects in difficult defect conditions [1, 2, 3, 4, 5]. Within this paper the authors wish to analyze the sizes dependence (voltages, currents) based on conditions the defect produces for establishing the possibility to selectively acknowledge the above mentioned defects. Furthermore, there are shown the technical characteristics of the protection block BZCD – 2, for analyzing the conditions when this protection block enables the selective acknowledgment of simple and double groundings in a bucking coil treated zero medium voltage.

II. Technical Considerations

A. Mathematic model for the analyze of a simple grounding

A.1) Theoretical consideration

The single phase circuit diagram for a (MVN) is shown in Fig. 1, where the notations have the following significance [2]: Tr – 110/20kV transformer; TSI – internal services transformer; Z_n – grounding impedance of the network; R_t – fault grounding resistance; L_1, L_2,…, L_n medium voltage electric lines [1, 2, 3, 4, 5].

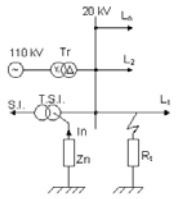

Fig. 1. Single phase circuit diagram for a (MVN) with simple grounding fault

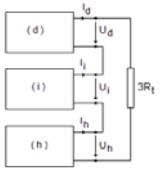

Fig. 2. Diagram for the connections of the sequences schemes for a simple grounding fault

Considering that the simple grounding fault occurs on the R phase of the MVN, the voltages and the currents in the fault area satisfy the following conditions [1, 2, 3]:

$$\underline{I}_S = \underline{I}_T = 0\ ;\quad \underline{U}_R = R_t \cdot \underline{I}_d \tag{1}$$

From the first equation of (1) results that the sequence schemes for the simple grounding fault are connected in series.

$$\underline{I}_d = \underline{I}_i = \underline{I}_h \tag{2}$$

The voltage at the fault is expressed by:

$$\underline{U}_R = 3 \cdot R_t \cdot \underline{I}_h \tag{3}$$

We consider that the three phased system of the supply is symmetrical in direct sequence, so that:

$$\underline{I}_{fault} = \frac{3 \cdot \underline{U}_f}{\underline{Z}_d + \underline{Z}_i + \underline{Z}_h} \tag{4}$$

In (4) U_f represents the voltage on the "R" phase before the fault occurred, and the impedances represent the sequence impedance seen from the fault location, also before the fault occurred. It can be accepted (because of the infinite power of the 110kV system) that the components are static and equilibrated and:

$$\underline{Z}_d = \underline{Z}_i = \underline{Z}_{Trd} + \underline{Z}_{Ld} = R_{fTr} + R_{fL} + j(X_{fTr} + X_{fL}) \tag{5}$$

The homopolar sequence impedance is:

$$\underline{Z}_h = 3 \cdot (R_t + R_p + jX_p) + \underline{Z}_{Ld} + \frac{(\underline{Z}_{TSIh} + 3 \cdot \underline{Z}_n) \cdot \underline{Z}_{Ch}}{\underline{Z}_{TSIh} + 3 \cdot \underline{Z}_n + \underline{Z}_{Ch}} = 3 \cdot (R_t + R_p + jX_p) + \tag{6}$$
$$+ R_{fL} + jX_{fL} + \frac{\left[R_{fTSI} + 3 \cdot R_n + j(X_{fTSIh} + 3 \cdot X_n)\right] \cdot \left(R_{fC} + jX_{fCh}\right)}{R_{fTSI} + 3 \cdot R_n + R_{fC} + j(X_{fTSIh} + 3 \cdot X_n + X_{fTSIh} + 3 \cdot X_n)}$$

In (6) the transformer 110/20kV is in Y/Δ connection and TSI transformer is in zig-zag connection on the medium voltage. The equivalent impedance of the MVN seen from the faulty point, as a function of the frequency is:

Dumitru Toader is professor at the University "Politehnica" of Timisoara (dumitru.toader@et.upt.ro).
Petru Ruset is Head of PG/PTD in Siemens S.R.L. Romania (petru.ruset@siemens.com)
Ioan Hategan is with SMART S.R.L. (ihategan@smarttm.ro)
Ioan Diaconu is the Director of the National Dispatching Centre of the Romanian Power Grid Company Transelectrica S.A.
Nicolae Pinte is with Pintel S.R.L.

978-1-4244-2235-7/09/$25.00 ©2009 IEEE

$$\underline{Z}_e = 2\cdot R_{fTr} + 3\cdot(R_t + R_p + R_{fL}) + j(3X_p + 3X_{fL} + 2X_{fTr})\cdot\frac{f}{50} + \frac{\left[R_{fTSI} + 3\cdot R_n + j(X_{fTSIh} + 3\cdot X_n)\cdot\frac{f}{50}\right]\cdot\left(R_{fC} + jX_{fCh}\cdot\frac{50}{f}\right)}{R_{fTSI} + 3\cdot R_n + R_{fC} + j(X_{fTSIh} + 3\cdot X_n)\cdot\frac{f}{50} + jX_{fCh}\cdot\frac{50}{f}} \quad (7)$$

A.2) Numerical results

For the total capacitive current of the network we take the values 100A; 50A; 25A; 15A; 10A; 5A. The initial phase of the homopolar capacitive impedance (φ angle of the medium voltage line and the group TSI together with the grounding impedance of the MVN) is varied from 80° to 90°. The results obtained are shown in table I for the homopolar capacitive impedance, in table II for the homopolar impedance of TSP+BC and in table III for the homopolar impedance of MVN seen from the fault point. From the three tables results that the value of the argument φ is very important for the value of the homopolar impedance.

TABLE I

VALUES OF HOMOPOLAR CAPACITIVE IMPEDANCE

α°	Ic = 100A	Ic = 50A	Ic = 25A	Ic = 15A
90	- j 346,41	- j 692,82	- j 1386	- j 2309
89	6,046 – j 346,36	12,09 – j 692,71	24,18 – j 1385	40,51 – j 2309
88	12,09 – j 346,20	24,18 – j 692,40	48,36 – j 1385	80,60 – j 2308
87	18,13 – j 345,94	36,26 – j 691,87	72,52 – j 1384	120,87 – j 2306
86	24,16 – j 345,57	48,33 – j 691,13	96,66 – j 1382	161,10 – j 2304
85	30,19 – j 345,09	60,38 – j 690,18	120,77 – j 1380	201,28 – j 2301
84	36,21 – j 344,51	72,42 – j 689,03	144,84 – j 1378	241,40 – j 2297
83	42,22 – j 343,83	84,43 – j 687,66	168,87 – j 1375	281,45 – j 2292
82	48,21 – j 343,04	96,42 – j 686,08	192,84 – j 1372	321,41 – j 2287
81	54,19 – j 342,15	108,38 – j 684,29	216,76 – j 1369	361,27 – j 2281
80	60,15 - j 341,15	120,31 – j 682,30	240,61 – j 1365	401,02 – j 2274

TABLE 2

VALUES OF Z_H FOR TSP+BC (SELF SERVICES COIL IN SERIES WITH THE COMPENSATION COIL)

α°	Ic = 100A	Ic = 50A	Ic = 25A	Ic = 15A
90	12 + j 346,40	12 + j 692,80	12 + j 1406	12 + j 2327
89	17,55 + j 346,35	24,04 + j 692,70	36,08 + j 1406	52,16 + j 2327
88	23,10 + j 346,21	36,08 + j 692,38	60,16 + j 1405	92,30 + j 2326
87	28,64 + j 345,96	48,11 + j 691,85	84,22 + j 1404	132,43 + j 2324
86	34,18 + j 345,63	60,13 + j 691,12	108,26 + j 1403	172,51 + j 2321
85	39,72 + j 345,19	72,14 + j 690,17	132,28 + j 1401	212,55 + j 2318
84	45,24 + j 344,66	84,13 + j 689,02	156,25 + j 1398	252,52 + j 2314
83	50,75 + j 344,03	96,09 + j 687,66	180,18 + j 1396	292,42 + j 2310
82	56,26 + j 343,31	108,03 + j 686,09	204,06 + j 1393	332,24 + j 2305
81	61,75 + j 342,49	119,94 + j 684,31	227,88 + j 1389	371,96 + j 2299
80	67,22 + j 341,57	131,82 + j 682,32	251,63 + j 1385	411,56 + j 2292

TABLE 3

VALUES OF Z_H OF THE HOMOPOLAR IMPEDANCE OF THE MVN

α°	Ic = 100A	Ic = 50A	Ic = 25A	Ic = 15A
90	10.000 – j 338,10	40.000 – j 626,15	159.900 – j 6.181	443.900 – j 15.630
89	5089 – j 167,65	13.290 – j 221,92	31.870 – j 464,27	88.480 – j 984,21
88	3414 – j 109,02	7970 – j 134,34	17.700 – j 209,74	49.150 – j 413,86
87	2570 – j 79,34	5694 – j 96,11	12.260 – j 131,92	34.030 – j 250,23
86	2061 – j 61,40	4431 – j 74,68	9377 – j 95,22	26.030 – j 176,09
85	1721 – j 34,39	3627 – j 60,97	7595 – j 74,05	21.080 – j 134,52
84	1478 – j 40,77	3072 – j 51,43	6384 – j 60,33	17.720 – j 108,13
83	1295 – j 34,29	2664 – j 44,42	5508 – j 50,72	15.290 – j 89,96
82	1153 – j 29,24	2353 – j 39,03	4844 – j 43,63	13.440 – j 76,72
81	1040 – j 25,19	2108 – j 34,77	4325 – j 38,19	12.100 – j 66,65
80	946,50 – j 21,86	1909 – j 31,31	3907 – j 33,87	10.840 – j 58,74

In table 3 are presented the values of the homopolar impedance of the MVN seen from the point of the fault, when the fault is produced on the medium voltage bar of the transformer station and the frequency is 50 HZ. In these calculations the resonant regime was considered. In order to obtain $Z_h(f)$, the equivalent homopolar impedance of the MVN seen from the fault location we gave to the frequency a variation in the domain [40Hz, 500Hz], using MathCAD. The graphic representation was made only till 150 Hz (the third harmonic) because above this value there are no significant changes. The following graphic representations are made for. From Fig. 9 results that the value of homopolar voltage is maximum at a frequency of 50Hz if the transition resistance at the defect location is higher than 10Ω. Beneath this value of the transition resistance at the defect location homopolar voltage has maximum value at a frequency superior to the one of 50Hz. From fig. 10 results that the value of the fault current is minimum at the frequency of 50Hz, which is natural since it was supposed that the network functions at resonance.

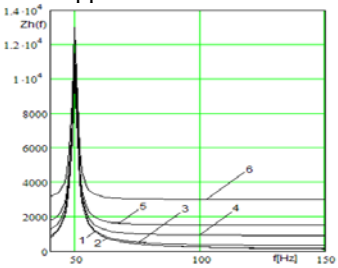

Fig. 3. Z_h (f) for Ic = 100A, φ = 90°, network at resonance

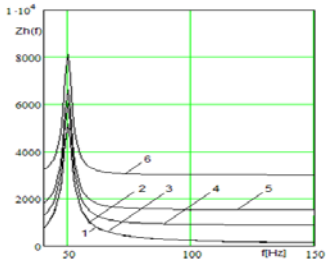

Fig. 4. Z_h(f) for Ic = 100A, φ = 89°, network at resonance

R_t = 0 Ω - curve 1, R_t = 10 Ω - curve 2 R_t = 100 Ω - curve 3 R_t = 300 Ω - curve 4 R_t = 500 Ω - curve 5 R_t =1000 Ω - curve 6.

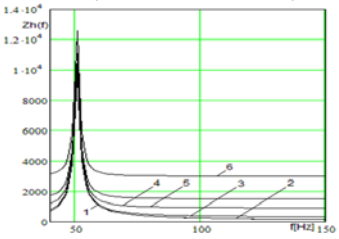

Fig.5. Z_h(f), Ic = 100A, φ = 90°, 10% overcompensated network

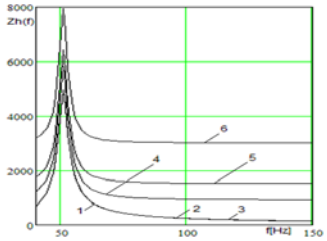

Fig. 6. Z_h(f) for Ic = 100A, φ = 89°, 10% overcompensated network

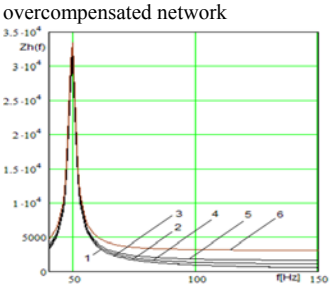

Fig. 7. Z_h(f), Ic = 25A, φ = 89°, network at resonance

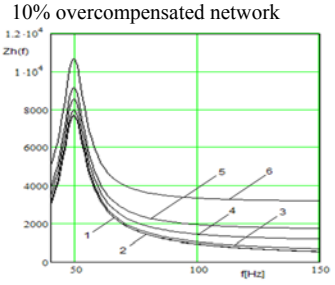

Fig. 8 Z_h(f), Ic = 25A, φ = 85°, network at resonance

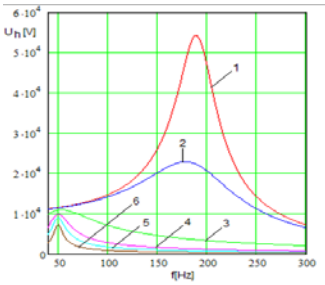

Fig. 9. U_h(f) for Ic = 100A, φ = 90°, network at resonance

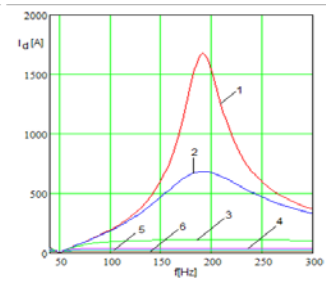

Fig. 10. I_d(f) for Ic = 100A, φ = 90°, network at resonance

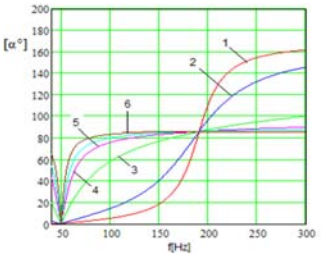

Fig. 11. Dependence of the homopolar voltage phase based on the frequency, for Ic = 100A, φ = 90°, network at resonance

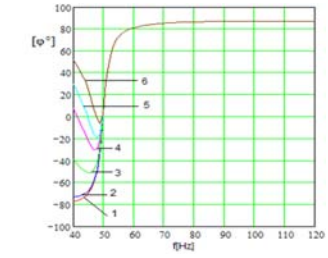

Fig. 12. Dependence of the phase difference between the homopolar voltage and the fault current based on the frequency, for Ic = 100A, φ = 90°, network at resonance

Fig. 11 shows that the phase of the homopolar voltage depends on the frequency, the maximum variation occurring

on zero fault location transition resistance. For $R_t = 0$ the phase of the homopolar voltage modifies within the period [0, 160°], and for $R_t = 1000\Omega$ it modifies within the period [0, 87°]. At 50Hz frequency the phase of the homopolar voltage is zero. The phase difference between the homopolar voltage and the fault current is depending on the transition resistance at the defect location value for the frequency of 50Hz and it is independent of it for higher frequencies.

From the analysis of the simple grounding defect result the following conclusions:

- The value of the homopolar capacitive impedance equivalent to the MVN seen from the fault point is strongly dependent on the quality of the insulation. If the insulation is older, the angle argument φ decreases and the resistance of the equivalent impedance increase. If the total capacitive current of the network is 100A, the growth of the resistance of the equivalent impedance goes till 6Ω if φ = 89°, till 12Ω if φ = 88°, till 18Ω if φ = 87°, till 30Ω till φ = 85° and till 60Ω if φ = 80°
- The resistive component of the homopolar impedance, equivalent to the TSI+BC group, depends on its argument similarly as the homopolar capacitive impedance of the MVN
- The value of the equivalent capacitive impedance of the MVN seen from the fault point depends in an important manner on the quality of the insulation. When insulation gets older, as mentioned above, the equivalent impedance decreases with 50% from the ideal value, if $I_c = 100A$, with 67% if $I_c = 50A$, with 80% if $I_c = 25A$, with 81% if $I_c = 15A$, with 90% if $I_c = 10A$ and with 95% if $I_c = 5A$.
- The most important dependence of the equivalent impedance on the frequency corresponds to the situation when the neutral point of the network is grounded trough compensation coil or if is isolated. For more than 100Hz the impedance reduces to the grounding resistance at the fault point.
- Only if the grounding fault resistance is lower than 10Ω the fault such as simple grounding can be detected if the neutral point of the network is isolated or is grounded trough compensation coil
- When the grounding resistance at the fault point is great, such a fault can be detected by checking the phase difference of homopolar currents versus the homopolar voltage of the medium voltage bars from the transformer station.
- When the grounding resistance at the point of the fault is very small the phase difference mentioned above is near to 90°. This implies o very low active power and by consequence the impossibility of using a wattmetric device in order to establish the faulty line.

One of the solutions to the last two conclusions is the Fourier analyze (to determine the harmonic content) of the homopolar current, the richest being that one of the faulty line.

B. Mathematical modeling of double line to ground faults

B.1) Theoretical consideration

A double line-to-ground fault in a medium voltage power network consists from two single line-to-ground faults which occurs either on two different lines of the same transmission line or on two lines of two different transmission lines. For such a fault the nonsymmetrical elements interconnect two different nodes (a_1, b_1) of the same symmetrical network with the symmetrical network equivalent to earth, whose parameters are zero. Such a fault is represented schematically in Fig.13, [2, 3, 7, 8, 9, 10, 11, 12].

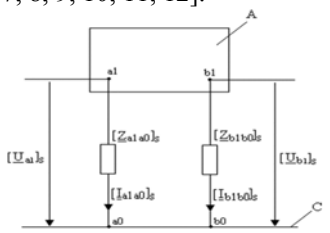

Fig.13 - Double line-to-ground fault

For this fault type eq.(8) becomes:

$$\begin{bmatrix} [\underline{U}_{ea1}]_S - [\underline{U}_{a1}]_S \\ [\underline{U}_{eb1}]_S - [\underline{U}_{b1}]_S \end{bmatrix} = \begin{bmatrix} [\underline{Z}_{a1a1}]_S & [\underline{Z}_{a1b1}]_S \\ [\underline{Z}_{b1a1}]_S & [\underline{Z}_{b1b1}]_S \end{bmatrix} \cdot \begin{bmatrix} [\underline{I}_{a1a0}]_S \\ [\underline{I}_{b1b0}]_S \end{bmatrix} \quad (8)$$

The voltages and the currents of nonsymmetrical elements which interconnect symmetrical networks can be expressed as follows:

$$[\underline{U}_{a1}]_S - [\underline{U}_{a0}]_S = [\underline{Z}_{a1a0}]_S \cdot [\underline{I}_{a1a0}]_S ; [\underline{U}_{b1}]_S - [\underline{U}_{b0}]_S = [\underline{Z}_{b1b0}]_S \cdot [\underline{I}_{b1b0}]_S \quad (9)$$

Assuming the earth potential to be zero, it follows that $[U_{a1}]_S - [U_{a0}]_S = [U_{a1}]_S$, respectively $[U_{b1}] - [U_{b0}]_S = [U_{b1}]_S$. As some of the entries of impedance matrix $[Z_{a1a0}]_S$ and $[Z_{b1b0}]_S$ are infinite, to compute the sequences we will proceed starting from the phase voltages at the fault location.

Expanding eq.(8) we get:

$$\begin{aligned} \underline{U}_{ea1h} &= \underline{U}_{a1h} + \underline{Z}_{a1a1h}\underline{I}_{a1a0h} + \underline{Z}_{a1b1h}\underline{I}_{b1b0h} \\ \underline{U}_{ea1d} &= \underline{U}_{a1d} + \underline{Z}_{a1a1d}\underline{I}_{a1a0d} + \underline{Z}_{a1b1d}\underline{I}_{b1b0d} \\ \underline{U}_{ea1i} &= \underline{U}_{a1i} + \underline{Z}_{a1a1i}\underline{I}_{a1a0i} + \underline{Z}_{a1b1i}\underline{I}_{b1b0i} \\ \underline{U}_{eb1h} &= \underline{U}_{b1h} + \underline{Z}_{a1b1h}\underline{I}_{a1a0h} + \underline{Z}_{b1b1h}\underline{I}_{b1b0h} \\ \underline{U}_{eb1d} &= \underline{U}_{b1d} + \underline{Z}_{a1b1d}\underline{I}_{a1a0d} + \underline{Z}_{b1b1d}\underline{I}_{b1b0d} \\ \underline{U}_{eb1i} &= \underline{U}_{b1i} + \underline{Z}_{a1b1h}\underline{I}_{a1a0i} + \underline{Z}_{b1b1i}\underline{I}_{b1b0i} \end{aligned} \quad (10)$$

From the physical conditions which the current must satisfy at the two fault locations, we get

$$\underline{I}_{a1a0h} = \underline{I}_{a1a0d} = \underline{I}_{a1a0i} ; \ \underline{I}_{b1b0d} = a\underline{I}_{b1b0h} ; \ \underline{I}_{b1b0i} = \underline{I}_{b1b0h} \quad (11)$$

The voltages at the fault locations can be expressed in terms of the symmetrical components as

$$\begin{aligned} \underline{U}_{a1} &= \underline{U}_{a1h} + \underline{U}_{a1d} + \underline{U}_{a1i} = 3\underline{Z}_{p1}\underline{I}_{a1a0h} \\ \underline{U}_{b1} &= \underline{U}_{b1h} + a^2\underline{U}_{b1d} + a\underline{U}_{b1i} = 3\underline{Z}_{p2}\underline{I}_{b1b0h} \end{aligned} \quad (12)$$

Equations (10), (11) and (12) yield the zero-sequence currents at the fault locations:

$$\underline{I}_{a1h} = \frac{\underline{U}_R\left(\underline{Z}_{b1b1h} + 2\underline{Z}_{b1b1d} + 3\underline{Z}_{p2}\right) - \underline{U}_S\left(\underline{Z}_{a1b1h} - \underline{Z}_{a1b1d}\right)}{\left(\underline{Z}_{a1a1h} + 2\underline{Z}_{a1a1d} + 3\underline{Z}_{p1}\right)\left(\underline{Z}_{b1b1h} + 2\underline{Z}_{b1b1d} + 3\underline{Z}_{p2}\right) - \left(\underline{Z}_{a1b1h} - \underline{Z}_{a1b1d}\right)^2} \quad (13)$$

$$\underline{I}_{b1h} = \frac{\underline{U}_S\left(\underline{Z}_{a1a1h} + 2\underline{Z}_{a1a1d} + 3\underline{Z}_{p1}\right) - \underline{U}_R\left(\underline{Z}_{a1b1h} - \underline{Z}_{a1b1d}\right)}{\left(\underline{Z}_{a1a1h} + 2\underline{Z}_{a1a1d} + 3\underline{Z}_{p1}\right)\left(\underline{Z}_{b1b1h} + 2\underline{Z}_{b1b1d} + 3\underline{Z}_{p2}\right) - \left(\underline{Z}_{a1b1h} - \underline{Z}_{a1b1d}\right)^2}$$

Referring to Fig.14, the impedances in eq.(13) can be expressed as follows:

$$\underline{Z}_{a1a1d} = \underline{Z}_{L1d} + \underline{Z}_{Trd};\quad \underline{Z}_{a1a1h} = \underline{Z}_{L1h} + \frac{\underline{Z}_{Ch}\left(\underline{Z}_{hBPN} + 3\underline{Z}_{BC}\right)}{\underline{Z}_{Ch} + \underline{Z}_{hBPN} + 3\underline{Z}_{BC}}$$

$$\underline{Z}_{b1b1d} = \underline{Z}_{L2d} + \underline{Z}_{Trd};\quad \underline{Z}_{b1b1h} = \underline{Z}_{L2h} + \frac{\underline{Z}_{Ch}\left(\underline{Z}_{hBPN} + 3\underline{Z}_{BC}\right)}{\underline{Z}_{Ch} + \underline{Z}_{hBPN} + 3\underline{Z}_{BC}} \quad (14)$$

$$\underline{Z}_{a1b1d} = \underline{Z}_{Trd};\ \underline{Z}_{a1b1h} = \frac{\underline{Z}_{Ch}\left(\underline{Z}_{hBPN} + 3\underline{Z}_{BC}\right)}{\underline{Z}_{Ch} + \underline{Z}_{hBPN} + 3\underline{Z}_{BC}}$$

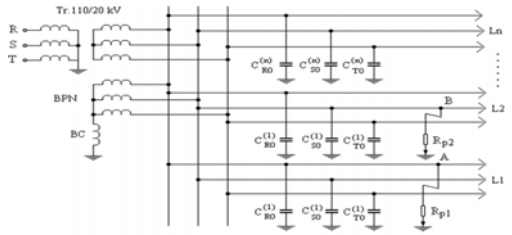

Fig.14 - Schematic diagram of a double line-to ground fault in a medium voltage network

The zero-sequence voltage on medium voltage substation bus bars can be expressed as follows:

$$\underline{U}_h = \frac{\underline{Z}_{Ch}\left(\underline{Z}_{hBPN} + 3\underline{Z}_{BC}\right)}{\underline{Z}_{Ch} + \underline{Z}_{hBPN} + 3\underline{Z}_{BC}}\left(\underline{I}_{a1h} + \underline{I}_{b1h}\right) \quad (15)$$

B.2) Numerical results

The results of the analysis were applied to a specific distribution network whose schematic diagram is shown in Fig.4. The sequence parameters of the network elements have the following values [14-17]: $\underline{Z}_{Trd}=\underline{Z}_{Tri}=(0{,}1+j2{,}1)\Omega$; $\underline{Z}_{BPNh}=(11+j28{,}5)\Omega$; $\underline{Z}_{Ch}=(12+j345)\Omega$; $\underline{Z}_{BC}=(2+j101)\Omega$; $\underline{Z}_{L1d}=\underline{Z}_{L1i}=(4+j3{,}5)\Omega$; $\underline{Z}_{L1h}=(5{,}5+j16{,}5)\Omega$; $\underline{Z}_{L2d}=\underline{Z}_{L2i}=\underline{Z}_{L2h}=0$; $\underline{U}_R=11547$ V; $\underline{U}_S=(-5773{,}5-j10000)$V; $R_{p2}=(1;\ 10;\ 50;\ 100;\ 500;\ 1000)\Omega$; $R_{p1}\in[0,\ 2000]\Omega$.

The operating regime of the 20 kV network has been assumed at resonance and the capacitive current of the network is 100 A. The first fault occurs at line L_1, at a distance of 10 km from the power station. The second fault occurs at the beginning of line L_2 and therefore the sequence impedances are zero.

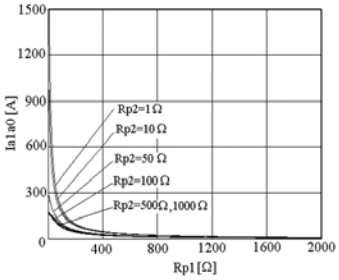

Fig.15 Fault current at first location (a_1)

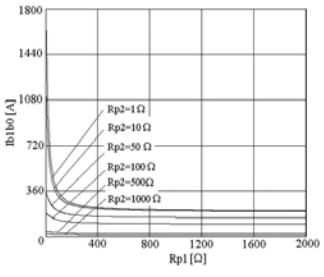

Fig.16 Fault current at second location (b_1)

In Fig.15 and 16 are shown the dependence of the fault currents as function of the fault resistance at location a_1, whereas the fault resistance at location b_1 is taken as a parameter. As can be seen, the two currents do not differ significantly so that in a first order approximation they can be considered equal.

Fig. 17 shows the dependence of the zero-sequence voltage at the output of the zero-sequence filter, as function of the fault resistance at location a_1 . It follows that if at one fault location the resistance is low (less than 10Ω) and at the other location the resistance is high (greater than 500Ω), the fault can be treated as a single-grounding fault. If at one location the resistance is grater than 1000Ω and at the other greater than 500Ω, than the zero-sequence voltage decreases below 10 V. Protective devices which senses zero-sequence voltage may not be able to detect the fault due to this low value.

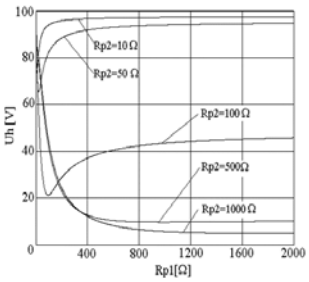

Fig.17 Zero-sequence voltage at the output of the zero-sequence filter

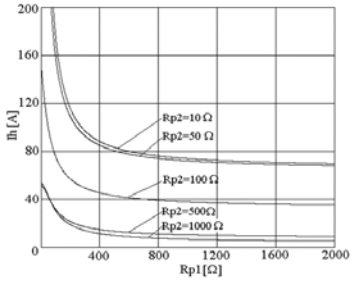

Fig.18 Zero-sequence current for faults on the same transmission line

In Fig.18 the dependence of the zero-sequence current of the faulty line is presented, assuming that both faults occur on the same transmission line. In this case, if the line's zero-sequence is controlled, again exists the risk of not detecting the fault.

From the performed analysis, the most important conclusions follow:

- the proposed network model allows to establish the way in which various parameters influences the zero-sequence voltage of the medium voltage bus bars, the fault currents, the zero-sequence of the faulty lines and the compensation reactor current;
- if the fault resistance at one location is less than 10 Ω and at the other location the fault resistance is greater than 500Ω, than the double-grounding can be treated as a single-grounding low-resistance fault;
- if the fault resistances at both locations are greater than 500Ω, than the zero-sequence voltage decreases below 15V; such a low value may not be detected by the protective devices;
- the value of the zero-sequence voltage is influenced by the fault resistance in such a way that the greater the resistances of the neutral-point and compensation reactors are, the greater this influence is; the same is true for the influences of the equivalent transversal conductance of the medium voltage network;
- if both faults occurs on the same transmission line, than the zero-sequence current of the line has a very low value even if the fault currents are high; therefore, if the protective device senses this current, there exists the risk of not identifying the faulty line.

The proposed mathematical model allows an easy analysis of double-grounding faults, no matter which quantity is chosen as independent variable. Single-groundings may also be analyzed with the proposed model by setting the fault resistance at one location to infinity.

C. BZCD – 2 Digital protection block

C.1) Generalization

BZCD-2 digital protection block is for the medium voltage networks with the neutral passed through the compensation reactor and performs the following functions: automat selective instantaneous and safe release of the medium voltage

line to metal simple groundings; automat selective instantaneous and safe release of the medium voltage line to double groundings. For assuring selective instantaneous and safe release of the MT line to simple and double groundings, BHAD-2 block comprises the following protections: frequency homopolar directional protection marked PHD for all simple groundings defects; homopolar current protection marked PHA against double grounding defects. Protection block contains a high computation speed performant microcontroller, RISC architecture allowing parallel programming, imposed by the phenomena analysis in real time. Moreover upon elaborating the software it has been considered that the number of instructions to be as small as possible [13, 14].

C.2) Block description

In fig. 19 is shown the main chart of the block and the connection mode in the protection charts.

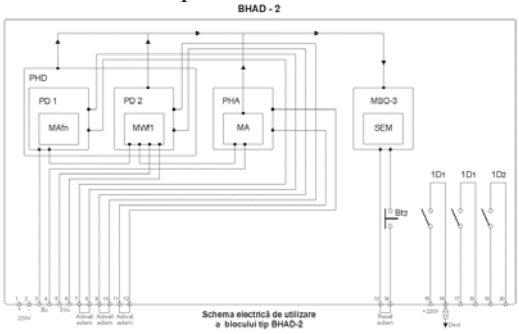

Fig. 19 Electrical chart of the protection block

Digital protection blocks comprise the following subassemblies:

Frequency directional homopolar protection marked with PHD in fig. 19, structured as follows:

- directional protection phase I, PD_1 (fig. 19) achieved from a frequency current module determining the frequencies higher than 50 Hz from the fault current, symbolized Maf_n in fig. 19 (f_n > 50 Hz), used for acknowledging simple grounding defects by low transition resistance (under 10Ω);
- directional protection phase II, PD_2 achieved from a frequency watt metric module de frequency de 50 Hz symbolized MWf_1 in fig. 19 (f_1 = 50 Hz), determining the homopolar current direction of the medium power lines, used for acknowledging simple grounding defects by high transition resistance (over 10Ω).
- homopolar current protection marked with PHA in fig. 19 containing an current module, used for used for acknowledging double grounding defects;

- optical signaling module marked with MSO-3 in fig. 19, activated by PD_1, PD_2 and PHA protections;
- the control module marked with MC in fig. 19 ($1D_1$), transmits the control for sending the defect lines switcher driving, by intermediary relay.

The above mentioned subassemblies are fitted in a box provided with adequate bridging-over terminals which must assure the connection of two conductors of 0.75 --- 2.5 smm each to the section.

C.3) Protection block settings

Case I: Simple grounding defect in the medium voltage network

When establishing the time settings for triggering PHD frequency directional homopolar protection are considered the following:

- The time necessary for blowing out the electric arc by the compensation reactor t_1 = 0.4---0.5 s;
- The time necessary for triggering directional protection stage I PD_1, $t_2 = t_1 + \Delta t$ = (0.4---0.5) + 0.2 = 0.6---0.7 s;
- The time necessary for triggering directional protection stage II PD_2, $t_3 = t_2 + \Delta t$ =(0.6---0.7) + 0.5 = 1.1---1.2 s.

When establishing the PD_1 and PD_2 protection triggering areas are considered the role of these protections.

In all cases when a simple grounding defect occurs in the medium voltage network, the homopolar voltage and current from FHC and FHT filters activates the measuring mode MAf_n or MWf_1 which after the expiring of the prescribed time performs the following operations: transmits the control for MC control module and the command to release the MT line switcher; transmits the command for memorizing the optical signaling on MSO-3 module.

a) Case II : A double grounding defect

When establishing the current settings for triggering PHA_k protection connected to FHC_k filter (homopolar current filter of L_k medium voltage line) are taken into consideration the following: maximum value of the permittance current of L_k medium voltage protected line ($I_{ck\ max}$); a safety coefficient K_{sig}= 1.5.

C.4) Technical characteristic of the block

- Feed circuit of BHAD-2 block with operative voltage (terminals 1-2 from fig. 19): Un = 220 Vcc.
- Directional protection stage I PD_1 performed with frequency current mode higher than 50 Hz MAf_n:
  - Graduated circle (terminals 3-4 from fig.19)
    - In = 5A, 50Hz
    - Imax = 50A, 50Hz
    - Imin = 10mA 150Hz
  - Time circuit
    - Optionally adjustable time scale for the following domain (0.2 --- 1 s)
    - Time error to temperature variations within the limits (-5ºC --- +40ºC) ±5%
  - Triggering circuit
    - Independent triggering terminals 7-8 from fig. 19, shunted
    - Exterior triggering is shunted terminals 7-8 from fig. 19, by the preset element
- Directional protection stage II PD_2 performed with frequency watt metric mode of 50Hz MWf_1:
  - Graduated circle (terminals 3-4 for current and 5-6 for voltage from fig. 19):
    - Un = 100V, 50Hz In = 5A, 50Hz
    - Umax = 110V, 50Hz Imax = 50A, 50Hz
    - Umin = 1V, 50Hz Imin = 20mA, 50Hz
    - Setting scale of the interior angle (represented in polar coordinates)
      - Corse setting: 0º, 45º, 90º, 315º;
      - Fine setting: 5º, 10º, 45º.

- The maximum sensitivity angle for the 20kV network with BC (represented in polar coordinates) φ_{max} = -10º corresponding to the 280º scale
- interior angle measuring error on temperature variations (-5ºC --- +40ºC) ±10%
- wattmetric module is not triggered at:
  - U = 100V 50Hz and I = 0A
  - U = 0V 50Hz and I = 50A

o Time circuit
- Optionally adjustable time scale for the following domain (0.5 --- 2.5 s)
- Time error to temperature variations within the limits (-5ºC --- +40ºC) ±5%

- Current homopolar protection achieved with current module MA

o Graduated circle (borne 3-4 from fig. 19)
- In = 5A, 50HzImax = 50A, 50Hz K_{min} > 0,95
- Optionally adjustable current scale for the following domain (0.2 --- 1A)
- error to measure temperature variations within the limits (-5ºC --- +40ºC) ±10%

o Time circuit
- Optionally adjustable time scale for the following domain (0.2 --- 1 s)
- time error at temperature variations within the limits (-5ºC --- +40ºC) ±5%

- Local signaling (within the block case) performed using LEDs at PD_1, PD_2, PHA and MSO-3
- Optical signaling resetting requirements

o Automat at 220 Vcc feed voltage impulse
- LED verde la PHD and PHA

o Manual by triggering a Bt_2 button fitted on the block case for deactivating red LED (T_1 ,T_2 ,T_3) at MSO-3
- Receiver circuit (with supplementary relay)

o Three n.d. contacts

o Rated voltage on contacts Un = 220 Vcc

o Currents on the terminals of the three contacts for n = 220 Vcc
- On shutting off 10A on starting 0.4A on a duration of 5A

C.5) Experimental determination

The presence of the compensation reactor in the primary circuit of the medium voltage network induces a significant decrease of the transitorial fault state, which produces great problems concerning protection sensibility. The intervention of the coil compensation current stabilizes a permanent fault state with a zero-sequence current with a very low value similar to the zero-sequence current measured in a normal state.

This disadvantage can be removed by adding a new module that controls higher frequency odd harmonics that are present in the first part of the transitorial state. This control is made by a so called "current harmonics module" was included as a constituent part of the current harmonics and zero-sequence power block BZCD 2, shown in Fig. 20.

Fig. 20 Protection block BZCD-2

The BZCD-2 protection block has been in the 220/110/6 kV Pestis plant using the scheme in Fig. 21, where:
- LES 6 kV PT Turn is connected to the second 6 kV line;
- The first 110/20 kV transformer is connected to the first 6 kV line;
- The CTv 6 kV transverse busbar is connected;
- The 6 kV LEA PT Turn switch is connected to the second 6 kV line;
- The 6 kV LEA PT Turn phase is ready to perform a single resistive grounding with values between 0,24 and 1 kΩ;
- The other consumers are connected to the first 6 kV line;
- For recordings we will use a CDR oscilloperturbograph.

During the tests, the BZCD-2 protection block has also been tested on the 6 kV PT Turn line, together with the maximum zero-sequence current protection, RDT.

To analyze the behavior of the protection block, the following single grounding tests have been performed for the 6 kV line:
- metallic grounding of a phase;
- grounding through the passing resistance R_t= 500 Ω;
- grounding through the passing resistance R_t= 1000 Ω.

Fig. 6.14 presents the electric scheme used for the Pestis plant tests. The evolution of voltages and currents as well as the transmission delay of triggering commands through the BZCD-2 block is shown in Fig. 21-24.

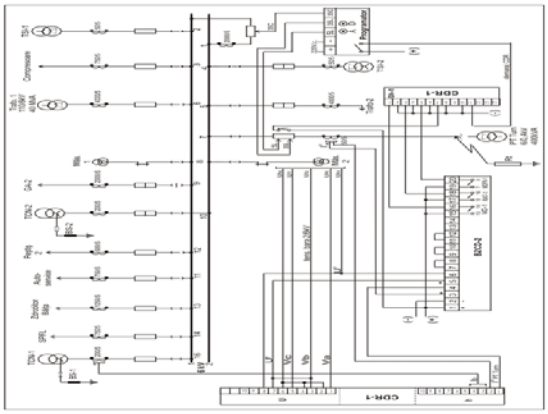

Fig. 21 Electric scheme used during the Pestis plant test

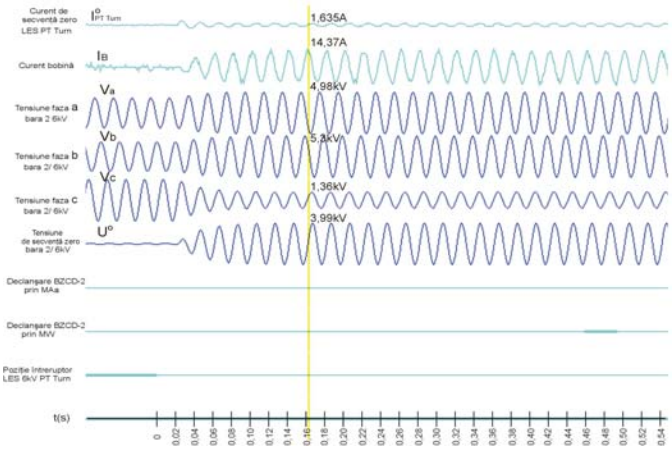

Fig.22. Single phase grounding R_t=1000 Ω, resonance tuning compensation coil

For compensation reactors with resonance tuning (I= 20 A), and a passing resistance for the fault location R_t=1000 Ω, one

can see that the zero-sequence fault current measured by the current transformer of the 6 kV PT Turn line has a 1,635 A value, or approximately 14% of the total current passing through the BC compensation reactor. The current direction (reverse in comparison to the coil) points to the fault line. One can notice that the fault current does not entirely return on the fault line, which clearly points to worn insulation on all galvanic connection lines of the Pestis plant. Voltage on the operating stages grows to 4,98 and 5,3 kV respectively. The triggering occurs at 0,44 s through the MW module.

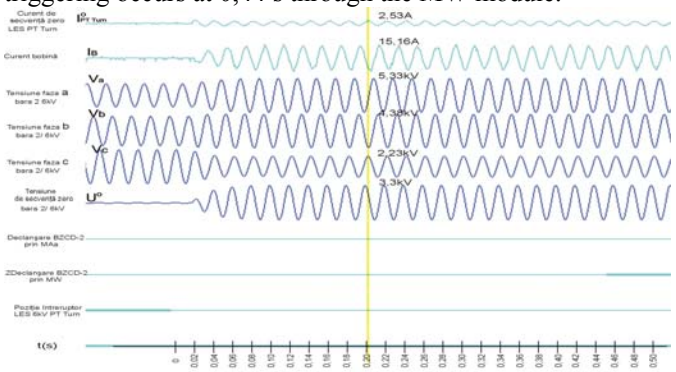

Fig.23. Single phase grounding with R_t=1000 Ω, and a 10% over-compensated compensation reactor

For under-compensated compensation reactors (I=18,5A) with a passing resistance at the fault location R_t=1000 Ω, the zero-sequence fault current measured by the current transformers of the 6 kV PT Turn line has a 2,53 A value, that is approximately 26,8% of the total current passing through the BC compensation reactor. The current direction (reverse in comparison to the coil) points to the fault line. Voltage on the operating stages grows to 5,35 and 3,73 kV respectively. The triggering occurs at 0,44 s through the MW module.

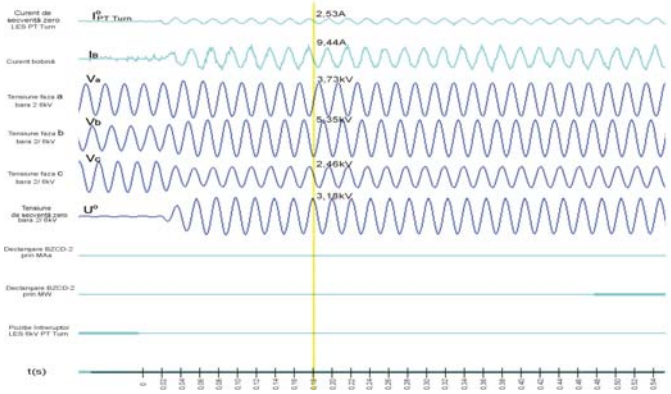

Fig. 24. Single phase grounding with R_t=1000 Ω, and a 10% under-compensated reactor

For resonance tuning compensation coils (I= 20 A), with a passing resistance at the fault location R_t=500 Ω, one can notice that the zero-sequence fault current measured by the current transformers of the 6 kV PT Turn line has a 1,94 A value, that is approximately 10,9% of the total current passing through the BC compensation reactor. The current direction (reverse in comparison to the coil) points to the fault line. Voltage on the operating stages grows to 5,52 and 5,6 kV respectively. The triggering occurs at 0,5 s through the MW module.

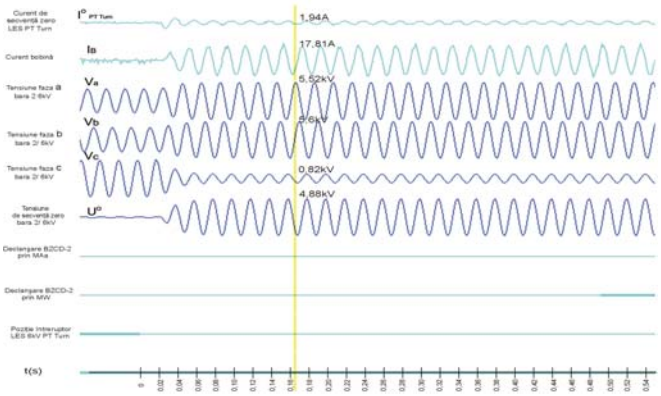

Fig. 25. Single phase grounding with R_t=500 Ω and a resonance tuning compensation coil

For overcompensating tuned reactors (I=23,5 A), with a passing resistance at the fault location R_t=500 Ω, one can notice that the zero-sequence fault current measured by the current transformers of the 6 kV PT Turn line has a 2,64 A value, that is approximately 13,5% of the total current passing through the BC compensation reactor. The current direction (reverse in comparison to the coil) points to the fault line. Voltage on the operating stages grows to 5,1 and 5,79 kV respectively. The triggering occurs at 0,5 s through the MW module.

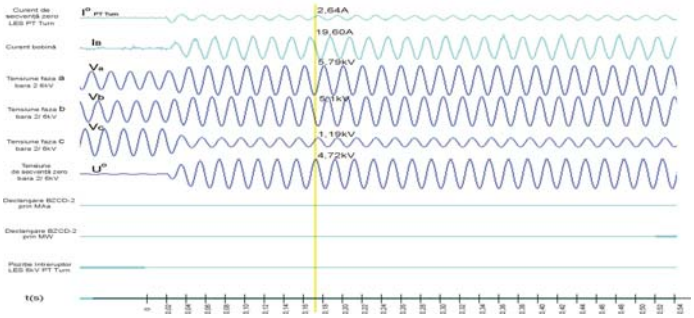

Fig. 26. Single phase grounding with R_t=500 Ω and a 10% over-compensated coil

For under compensating tuned reactors, with a passing resistance at the fault location R_t=500 Ω (I=18 A), one can notice that the zero-sequence fault current measured by the current transformers of the 6 kV PT Turn line has a 2,05 A value, that is approximately 11,5% of the total current passing through the BC compensation reactor. The current direction (reverse in comparison to the coil) points to the fault line. Voltage on the operating stages grows to 5,33 and 5,71 kV respectively. The triggering occurs at 0,5 s through the MW module.

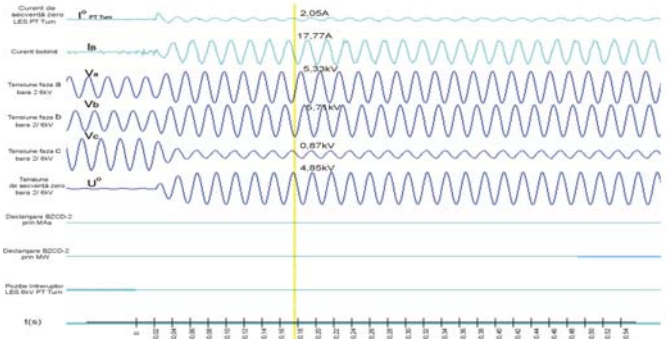

Fig. 27. Single phase grounding with R_t=500 Ω, and a 10% under-compensated reactor

For compensation reactors with resonance tuning (I=20 A) and a passing resistance for the fault location R_t=0 Ω, one can see that the zero-sequence fault current measured by the current transformer of the 6 kV PT Turn line has a 2,28 A value, or approximately 8,7% of the total current passing through the BC compensation reactor. The current direction (reverse in comparison to the coil) points to the fault line. Voltage on the operating stages grows to 6,15 and 6,22 kV respectively. The triggering occurs at 0,3 s through the MAa module, due to the transitorial state of the first semi-period.

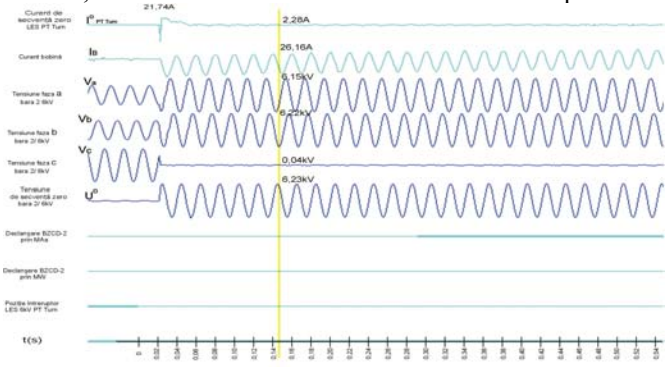

Fig. 28. Single phase grounding R_t=0 Ω, resonance tuning compensation reactor

For over-compensated tuning reactors (I=23,5 A), with a passing resistance at the fault location R_t=0 Ω, one can see that the zero-sequence fault current measured by the current transformers of the 6 kV PT Turn line has a 2,2 A value, that is approximately 8,2 % of the total current passing through the BC compensation reactor. The current direction (reverse in comparison to the coil) points to the fault line. Voltage on the operating stages grows to 6,16 and 6,24 kV respectively. The triggering occurs at 0,3.

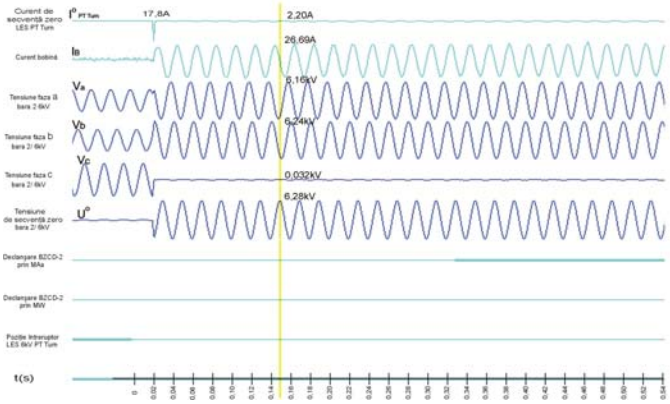

Fig. 29. Single phase grounding R_t=0 Ω, and a 10% over-compensated coil

For under-compensated tuning reactors (I=18,5A), with a passing resistance at the fault location R_t=0 Ω, one can see that the zero-sequence fault current measured by the current transformers of the 6 kV PT Turn line has a 2,5 A value, that is approximately 10,9% of the total current passing through the BC compensation reactor. The current direction (reverse in comparison to the coil) points to the fault line. Voltage on the operating stages grows to 6,15 and 6,2 kV respectively. The triggering occurs at 0,3 s through the MAa module.

The recorded oscillograms show the following:

- the total network permittance current has a value of $\sum I_C$ =20 A.
- for the metallic grounding of a phase over voltage on the operating phases grows by $\sqrt{3}$ times;
- during all phase grounding tests, the protection mechanisms of the BZCD-2 block sent the triggering command according to the adjustment calculated by t=0,3-0,5 s.

It is therefore noted that the new BZCD-2 protection block operates correctly in all cases, which proves the selectivity and safety of its protections. They act as they were designed to, both on the harmonics and on the power segment.

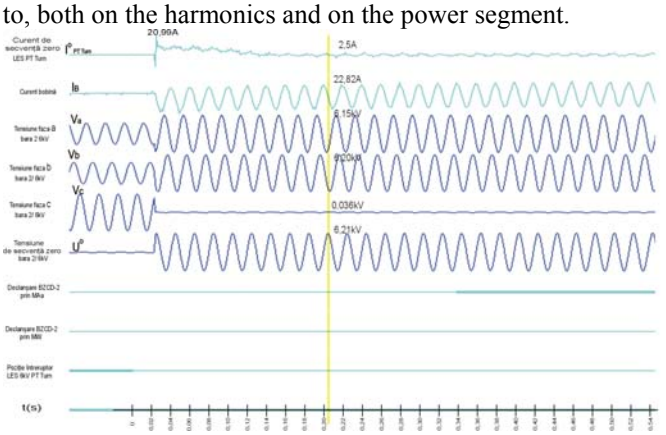

Fig. 30. Single phase grounding with R_t=0 Ω, and a 10% under-compensated reactor

D) Conclusions

The main conclusions resulting from the study are the following:

- The parameters intervening in the electrical chart equivalent to a medium voltage power network, as well as their values, depended mainly on the aging state of the insulation.
- On a medium voltage power network with aged insulation (angle of high value losses) cross conductibility becomes important (cannot be neglected anymore) due to resonance state is difficult to establish and the value of the value of the homopolar impedance decreases significantly even though the resonance state was achieved.
- A simple grounding defect low value transition resistance (under 10Ω) can be selectively acknowledge from the content of the harmonic module of the fault current.
- The content of the fault current harmonic decreases instantly when the value of the fault location resistance increases which is why the acknowledgement of a simple grounding by high transition resistance can be achieved selectively by controlling the direction of the homopolar currents afferent to the medium voltage lines connected to the same bars system.
- A double grounding defect and in case of a transition resistance to one of the defect locations or in both high value defect locations can be selectively acknowledged by controlling the value of the homopolar current of the medium voltage lines connected to the same bars system.
- BZCD – 2 digital protection blocks contains the protections necessary for selective acknowledgment of simple and double groundings. Due to high sensitivity it allows the acknowledgment of these defects in difficult defect

conditions, which represents an important step regarding the possibility to detect these defects.

- The experimental verifications performed on the real medium voltage power networks have proved that the elements considered when designing and achieving the digital protection block BZCD – 2 were correct.
- All the defects caused in the experimental sector achieved (Pestiş transformer plant) have been acknowledged correctly by the digital protection block BZCD – 2.

From the subjects presented above results that the digital protection block BZCD – 2 offers the possibility of simple and double grounding selective acknowledgement in medium voltage power networks. By equipping the protection installations afferent to the medium voltage lines with the mentioned block is solved one of the problems which represented the concern of a large number of electro-energetic researchers.

III. References

Periodicals:

[1] Ed. Clarke, *Analysis of the electro-energetic circuits and systems*, Technical Publishing House, Bucharest, 1973

[2] D. Toader, St. Haragus, "Analysis of Multiple Faults in Three-phase Network", Revue Roumaine de Science Techniques, Serie Electrotechniques et energetique, Tome 48, nr.2-3, 2003, p. 291-305.

[3] D. Toader, St. Haragus, C. Blaj, "Detection of broken conductor with ground contact faults in medium voltage power networks" Facta Universitatis series Electronics and Energetic Vol. 19, No. 3, December 2006, University of Nis, p. 429-438

[4] D. Toader, Şt. Hărăguş, The influence of operating regime on the voltages and currents in a medium voltage distribution network during a single-grounding fault, Acta Cibinienssis, Electrotechnics, Electronics and Computer Science, p.5-12, (1998).

Books:

[5] M. Eremia, a.o., *Electric Power Systems*, *vol.1, Electric Networks,* Academia Ed. Bucuresti, Romania, 2006

[6] D. Toader, St. Haragus, C. Blaj, *Analysis of Nonsymmetrical Medium Voltage Electric Network*, Politehnica., Ed. Timisoara, Romania, 2008.

Technical Reports:

[7] D. Toader, Şt. Hărăguş, Computation of capacitive currents of the healthy lines in the case of a single-grounding fault, Analele Univ. Oradea, p.27-33, (1997).

[8] D. Toader, Şt. Hărăguş, Analysis of Double-grounding faults in 20 kV Power Networks Neutral-point Grounded via a Compensation Reactor, An. Univ. Oradea, p.150-156, (2001).

[9] D. Toader, Şt. Hărăguş, Computation of capacitive currents of the healthy lines in the case of a single-grounding fault, Analele Univ. Oradea, p.27-33, (1997).

Papers Presented at Conferences:

[10] D. Ebehard and E. Voges, "Digital single sideband detection for interferometric sensors," presented at the 2nd Int. Conf. Optical Fiber Sensors, Stuttgart

[11] K. M. Winter "La compensation des courants résiduels – un procédé nouveau pour la protection des réseaux de câbles souterrains ou aériens contre les défauts a la terre" *MNT 95*, Mulhouse, Nov. 1995.

Papers from Conference Proceedings (Published):

[12] I. Diaconu, I. Hațegan, N. Pinte, D. Toader, "The Protection block for Medium Voltage Networks" Proceedings of the 2nd International Conference on Modern Power Systems – MPS 2008, Cluj – Napoca, p. 91-94.

[13] D. Toader, C. Blaj, St. Haragus, "Electrocution Danger Evaluation for Broken and Grounded Conductor" Proceedings of the Eurocon 2007 Conference September 9-12, 2007, Warsaw, Poland, p. 1392 – 1396.

[14] D. Toader, Şt. Hărăguş, V. Toaxen, *An Improved Method for Neutral-point Grounding in a Distribution Network*, Proc. IASTED Intern. Conf. on PES, Spain, p.28-131, (2000).

Dissertations:

[15] D. Toader, Contributions regarding the study of the "grounded and broken wire" defects in the medium voltage electric networks, Doctoral dissertation, I.P. Timişoara, 1986.

[16] I. Diaconu, Contributions regarding conceiving the protections from the medium voltage electric networks with the neutral grounded trough compensation coil. Doctoral dissertation Polytechnic University of Bucharest, 2008.

IV. Biographies

Dumitru Toader has a B.Sc. in electrotechnics from the Politechnical Institute "Traian Vuia" of Timisoara in 1971. Between 1971 – 1975 he was a research engineer at
"Industrial Station Power Networks of Bucharest", "Protection and Automation Laboratory of Deva". Currently is professor of Timisoara University of Polytechnics.

Ion Petru Ruset was born on June 29, 1964. He has a B.Sc. in general electrotechnics from the University of Timisoara, Faculty of Electrotehnics in 1989, PhD study for General Electrotechnics at Timisoara University. He has seventen years of experience in the HV substation transformer 400,200MVA, primary equipment, and automation and protection systems. Between November 1998 and June 2007, he was Technical Manager of the Romanian National Transmission Company - Transelectrica, Service for Transmission Grid Romania – Smart Timisoara. Since July 2007, he has been the Head of PG/PTD in Siemens s.r.l. Romania.

Ioan Dorin Hategan was born in 1955 may 8 in Blaj, Romania. He received the EE Engineering from the Politechnical Institute of Bucharest in 1980, and the Ph. D. degree in electrical engineering from the Technical University in Timisoara in 2004. Currently is working in Romanian Power Grid in CNTEE Transelectrica SA as Head of Technical Department. CIGRE and IEEE member.

Nicolae Florean Pinte was born in Băbeni (Romania), on June 15, 1964. He graduated from the Bucharest Institute of Polytechnics in 1988. He worked at ICPE (Research and Engineering Institute for Electrical Engineering) in Bucharest between 1995 and 2000. Since 2000, he has been Executive Manager at Pintel Intelligent Systems Bucharest. He has 7 patents for automation inventions. He is the author of TIS (Theory of Informational Species-*Irecson* Publishing House, Bucharest, 2007) and of more than 20 technical papers.

Ioan Diaconu has recently been appointed director of the Operational Unit of the National Dispatch Center, after having formerly been Director General and Chairman of the Board of Directors for CN Transelectrica SA – SC "Smart" SA Subsidiary between 2001 – 2009.
He had previously been a specialist, energy dispatcher and head of dispatching shift at the Control Room of the National Dispatch Center – CN Transelectrica SA.
Mr. Ioan Diaconu is a Ph. D. and was awarded several expert certificates such as: Technical Execution Expert, Design Supervisor, Extra-Judicial Technical Expert, Work Conductor for Live Work at 220-400 kV OHLs.